J. Biochem. 2014;1–10 doi:10.1093/jb/mvu073 Journal of Biochemistry Advance Access published December 8, 2014 THE JOURNAL OF BIOCHEMISTRY

Quantitative analysis of the interaction between L-methionine derivative and oligonucleotides

Received July 28, 2014; accepted September 29, 2014; published online November 24, 2014

Élia Mota, Fani Sousa, João A. Queiroz and Carla Cruz*

CICS-UBI – Centro de Investigação em Ciências da Saúde, Universidade da Beira Interior, Av. Infante D. Henrique, 6200-506 Covilhã, Portugal

*Carla Cruz, CICS-UBI – Centro de Investigação em Ciências da Saúde, Universidade da Beira Interior, Av. Infante D. Henrique, 6200-506 Covilhã, Portugal. Tel: +351 275 329 097, Fax: +351 275 329 099, email: carlacruz@fcsaude.ubi.pt

This study explores the use of L-methionine derivative as a potential affinity ligand for nucleic acids purification. The L-methionine derivative is synthesized by activation of the carboxylic acid group with 1-ethyl-3-(3-dimethylaminopropyl) carbodiimide/*N*-hydroxysuccinimide follow by immobilization on amine sensor surface, previously activated and treated with ethylenediamine. Their affinity towards oligonucleotides has been determined by surface plasmon resonance biosensor. The highest affinity is found for cytosine and thymine, followed by adenine, whereas the lowest affinity is found for guanine. For hetero-oligonucleotides the affinity order is CCCTTT > CCCAAA ≈ AAATTT > GGGTTT, showing that nucleotides with cytosine have the highest affinity, and the presence of guanine reduces the affinity, corroborating with the results obtained with homo-oligonucleotides.

Keywords: binding interactions/L-methionine/oligonucleotides/surface plasmon resonance.

Abbreviations: RU, resonance units; SPR, surface plasmon resonance.

Nucleic acids and proteins are two different macromolecules interacting constantly in cellular processes. Specific nucleic acid–protein interactions are the basis of cell life because numerous biological mechanisms depend on it such as replication, transcription, splicing and DNA repair (*1–5*). Despite decades of research, it is not yet clear whether there are a general 'recognition code' dictating the specificity of the interaction between amino acids and nucleotide bases (*6*, *7*). The knowledge of the groups of atoms involved is relevant to predict the type of favoured intermolecular interactions. The three-dimensional structures of numerous protein–DNA complexes determined by X-ray crystallography and nuclear magnetic resonance (NMR) spectroscopy have been extensively analysed, providing a basic representation of the way that these two macromolecules interact (*8–11*). The proteins present domains able to recognize specific DNA sequences (*12*). The most frequent interactions are the hydrogen bonds, followed by van der Waals, hydrophobic and electrostatic interactions (*2*).

Amino acids-DNA affinity chromatography has been widely used (*13*, *14*) to purify supercoiled (sc) plasmid DNA (pDNA). This affinity technique to purify plasmids can be safely used once is based in the natural occurrence of interactions between proteins and nucleic acids.

Despite the ligands with biological origin tend to be fragile and associated with low binding capacities (*15*), several advantages, such as, the high specificity and efficiency of affinity interactions are crucial if a single chromatographic step is required, allowing increased yields and improved process economics (*16–19*). Affinity is determined by the chemical complementation between a protein and a DNA sequence (*20*). The isothermal titration calorimetry and surface plasmon resonance (SPR) are examples of techniques that provide binding information about protein–DNA interactions in thermodynamic and kinetic approaches (*14*, *21*).

The analytical concept of affinity chromatography is the analysis of the interactions of mobile molecules flowing over surface-immobilized ligands (*2*) which can be mimicked in the SPR biosensor, allowing the characterization of affinity events and real-time monitoring of binding kinetic (*22*, *23*). Furthermore, short chain oligonucleotides, with several specific sequences, are attractive models to study the interactions with amino acids as they allow a clear interpretation of the experimental data (*24*) and an estimation of the binding with more complex nucleic acids.

L-methionine was chosen as a model since is a hydrophobic amino acid with a sulphur atom in its side chain that mediates a larger number of contacts in protein–nucleic acid interactions (*25*) and is different from those that have been previously studied by our group (*26–29*).

A preliminary study to screen specific interactions between L-methionine-agarose support and 5′-mononucleotides was done by chromatographic experiments and by saturation transfer difference (STD)-NMR spectroscopy (*30*). In this support the amino acid has the carboxylic group free to interact with 5′-mononucleotides. In this preliminary study, the STD-NMR results revealed that hydrophobic residues (CH_3 of thymine and adenine) can preferentially interact with the L-methionine side chain of the support. In addition, uridine 5′-monophosphate, cytidine 5′-monophosphate and guanosine 5′-monophosphate interact with the support mainly through the sugar-phosphate backbone. Moreover, thymidine 5′-monophosphate led to more contacts with the L-methionine support and also

had the highest retention time in chromatographic studies. Larger homo-oligonucleotides that have more hydrophobic bases had higher retention time, *i.e.* higher contact with L-methionine support (*30*).

Herein, L-methionine derivative is synthesized, characterized and immobilized on amine surface of the chip. In this case, the amine group is free to interact with different oligonucleotides sequences. The equilibrium constants are estimated, and their binding preferences are established to improve molecular recognition in a chromatography experiment using this amino acid derivative.

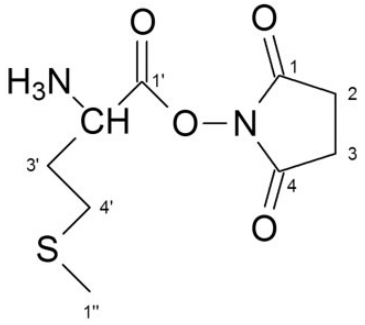

Fig. 1 Chemical structure of L-methionine derivate.

Materials and Methods

All solutions were freshly prepared using deionized water ultra-pure grade, purified with a Milli-Q system from Millipore (Billerica, MA, USA). The buffers were filtered through a 0.20 µm pore size membrane (Schleicher Schuell, Dassel, Germany). SPR analysis was performed using a Biacore T200 system (GE Healthcare Biosciences, Uppsala, Sweden) equipped with a carboxymethyl dextran sensor chip (CM5) and controlled by Biacore T200 Control Software. The series S sensor chip CM5, BIA normalizing solution (70% glycerol), amine-coupling kit [*N*-hydroxysuccinimide (NHS), *N*-ethyl-*N*′-(3-diethylaminopropyl)carbodiimide hydrochloride (EDC), 1 M ethanolamine-HCl], HBS-N buffer (10 mM HEPES pH 7.4, 150 mM NaCl) and HBS-EP buffer (10 mM HEPES pH 7.4, 150 mM NaCl, 3 mM EDTA, 0.005% v/v Surfactant P20), immobilization buffer (10 mM sodium acetate pH 5.0) and P20 surfactant were purchased from Biacore (GE Healthcare Biosciences). L-methionine, 2-(*N*-morpholino)ethanesulfonic acid (MES), Tris–HCl and borate buffers were purchased from Sigma-Aldrich (St. Louis, MO, USA). Single-strand oligonucleotides were provided by Primm (Milano, Italy) and stored at −20°C. Working solutions at various concentrations were freshly prepared using the running buffer solution (10 mM Tris–HCl pH 8.0, 0.005% v/v Surfactant P20).

Synthesis and characterization of ligand

The L-methionine derivative was obtained by activation of the carboxylic acid group with EDC/NHS. Briefly, L-methionine (0.239 g, 0.4 M) was dissolved in 4 ml of 100 mM MES at 50°C. Then, 1 ml of 1:1 mixture of 0.48 M NHS and EDC was added dropwise to the previous solution, stirred for 24 h at 50°C and then heated to reflux for 1 h. The solvent was removed under reduced pressure, and the resulting residue was treated with ethanol at 50°C. The white solid formed was filtered off, and the solvent was evaporated under reduced pressure. The pure compound was precipitated from acetonitrile solution as a white powder and dried. Finally, the desire compound was characterized by NMR spectroscopy (see Fig. 1 and Table I).

The ^{1}H and ^{13}C NMR spectra were recorded in D_2O solution at temperature of 298 K on a Bruker Avance III 400 MHz spectrometer operating at 9.4 T observing ^{1}H at 400.13 MHz and ^{13}C at 100.62 MHz. The spectrometer was equipped with a BBFO (broad band) probe, and all spectra were acquired and processed with the software topspin 3.1. Chemical shifts are reported in ppm using sodium trimethylsilyl propionate-d_4 as an internal standard.

Immobilization of the L-methionine derivative

Experiments were performed using a Biacore T200 equipped with a CM5 sensor chip (series S). The system was prepared with HBS-N buffer, 0.005% P20 on the left-hand tray and deionized water on the right-hand tray. The detection was conducted at 25°C. After docking the sensor chip, the detector was normalized with BIA normalizing solution to compensate for slight differences in detector responses between individual sensor chips.

The immobilization of L-methionine derivative on the CM5 sensor chip involved two steps. First, the carboxymethyl dextran matrix of a CM5 chip was activated by injection of EDC and NHS (70 µl, 200 mM EDC, 50 mM NHS) for 7 min at a flow rate of 5 µl/min, which leads to the formation of succinimide esters. These were treated with a solution of ethylenediamine (50 µl, 1 M in 100 mM borate buffer, pH 10.15) to generate a surface bearing free amine groups (*22*, *26*). Then, the L-methionine derivative at concentration of 0.5 M in 10 mM acetate pH 5.0, was immobilized in flow cell 2 by reacting with the -NH_2 groups of ethylenediamine forming an amide bound between the sensor chip and the ligand (see Scheme 1).

Table I. ^{1}H and ^{13}C NMR spectral data of L-methionine derivative[a] (D_2O, 400 MHz).

Position[b]	δ_C DEPT135 (ppm)	δ_H (ppm), multiplicity
1 and 4	177.1 (C)	
2 and 3	44.1 (CH_2), 60.4 (CH_2)	3.15 *t*, 3.82 *t*
1′	188.6 (C)	
2′	56.8 (CH)	3.87 *m*
3′	32.5 (CH_2)	2.20 *m*
4′	31.7 (CH_2)	2.65 *t*
1″	16.8 (CH_3)	2.14 *s*

[a]Assigned by COSY, HMBC and HSQC experiments.
[b]See Figure 1.

The immobilized density averaging was 122.5 resonance unit (RU). The flow cell 1 act as a blank, on which no ligand was immobilized to minimize variations caused by non-specific binding and bulk refractive index changes. All the surfaces were blocked with a 7 min injection of 1 M ethanolamine pH 8.0, followed by HBS-N injection to stabilize the baseline (see Scheme 1). HBS-N was used as a running buffer during immobilization. The running buffer circulates through the circuitry and avoids the accumulation of the amino acid on the walls of the fluidic system.

SPR measurements

All binding experiments were carried out at 25°C in 10 mM Tris–HCl pH 8.0, 0.005% v/v Surfactant P20 as running buffer. Once the L-methionine coated sensor chip was stable in the running buffer the solutions containing the analytes (homo- and hetero-oligonucleotides) were passed over the two flow cells at flow rate 2 µl/min. The concentrations injected of nucleotides with distinct molecular masses (3, 6, 15 and 30) ranged between 22.9 and 0.004 mM and for hetero-oligomers ranged between 11.3 and 0.02 mM. Aliquots of each concentration were transferred into separate 7-mm Biacore tubes for duplicate analysis of the concentration series. The 2× Tris–HCl 7-mm tubes were also used to serve as blanks. Caps were placed on top of the 7-mm tubes to minimize sample contamination and evaporation.

Duplicate injections of each sample were injected over the L-methionine and reference surfaces, in the order of decreasing concentration. No regeneration solution was required as all oligonucleotides were removed from the sensor surface. In addition, blank injections (running buffer without analyte) were performed prior to each collection of binding data following exactly the same time course as the runs with analyte. Subtraction of the response of the blank injections from the data traces (double referencing) corrects for unspecific binding of oligonucleotides to the sensor chip, instrument drift and refractive index changes as well as signal noise caused by oligonucleotides injections (single referencing). Steady-state binding studies were carried out by averaging the RU values in the plateau region of the sensorgrams over a 300–400 s period. All data processing and analysis were performed using Biacore T200 Evaluation Software v. 1.0. The equilibrium constant

was obtained by fitting plots of RU versus concentration of analyte ([analyte]). The data were fitted to a bimolecular interaction model, yielding a single equilibrium dissociation constant, K_D ($R_{eq} = K_A \times [analyte] \times R_{max}/(1 + K_A \times [analyte] \times n)$). The K_D was estimated when the Chi-square values were minimized.

Results and Discussion

To optimize specific binding to L-methionine chromatographic support, we studied oligonucleotides binding to L-methionine–coated surface using the SPR biosensor.

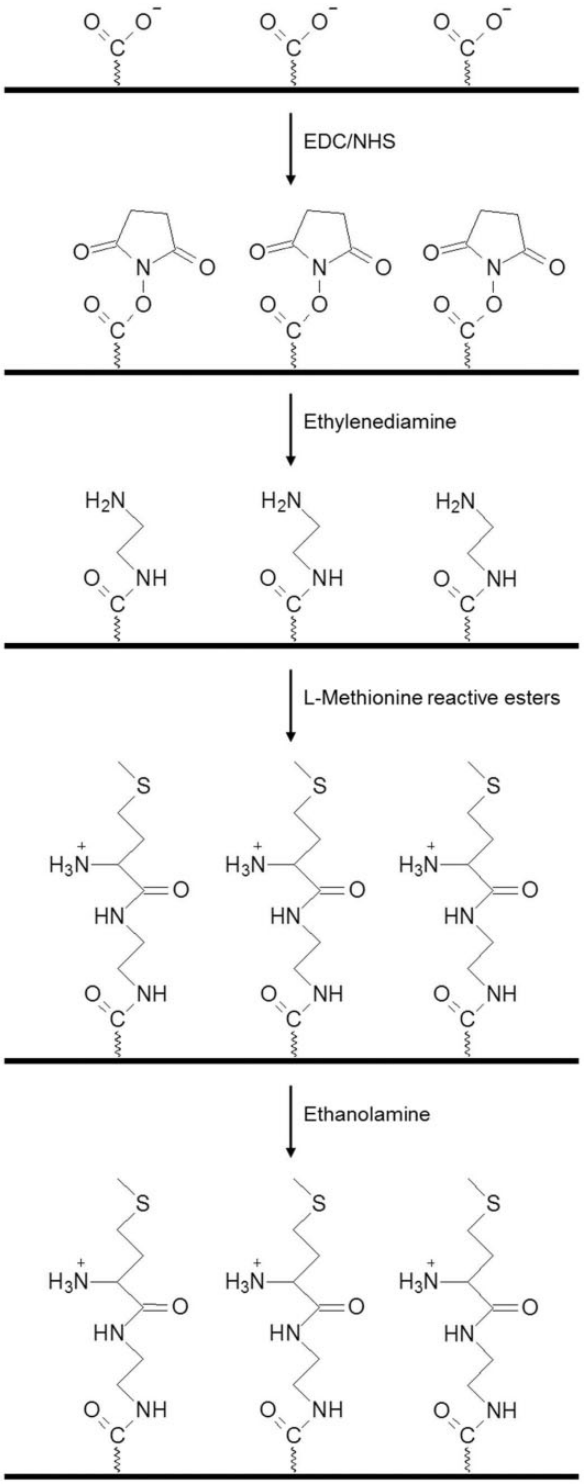

Scheme 1 L-methionine immobilization on the chip surface.

To set up the SPR binding assays, the L-methionine derivative was synthesized by activation of the carboxylic acid group with EDC/NHS followed by immobilization on amine sensor surface, previously activated with ethylenediamine. This strategy was done to verify if the amine group is preferential for the binding to the oligonucleotides instead of the carboxylic group. The K_D values of each single strand of polyA (6, 15 and 30), polyC (3, 6, 15 and 30), polyG (*15*) and polyT (3, 6, 15 and 30 nucleotides) and also A AATTT, CCCTTT, CCCAAA and GGGTTT to the immobilized L-methionine were determined. The homo-oligonucleotides were chosen due to their different size, and the hetero-oligonucleotides were chosen due to their different bases composition. Hence, this work allows studying the effect of the oligonucleotides molecular mass and the hydrophobic character of the individual bases on the interactions to L-methionine surface, to evaluate the binding preferences of the bases.

The affinity data are obtained at $T = 25°C$, and the running buffer used was 10 mM Tris–HCl pH 8.0 containing 0.005% of surfactant P20. The binding responses were detectable and reproducible. Sensorgrams obtained were identical for all complexes despite the low resonance response levels achieved, with all the oligonucleotides saturation of the active surface ranging approximately between 15.4 and 264.9 RU (normalized signal).

To further characterize the influence of molecular mass and bases composition in ligand–analyte interactions in a quantitative mode, R_{eq} values were estimated from the non-linear fitting by averaging the RU values at the plateau region of the sensorgrams over a 300–400 s. Plotting R_{eq} against free oligonucleotide concentration, Langmuir binding isotherms were obtained. The SPR binding profiles obtained were markedly square shaped responses, indicating that k_{on} and k_{off} could not be estimated.

The K_D values of each oligonucleotide are presented in Table II. There are few differences in the apparent affinity correlated with different oligonucleotides. All K_D values are in the submM range. The

Table II. Equilibrium analysis of the oligonucleotides performed at 25°C.

Oligonucleotide	K_D (M) ± SD
A_6	$5.52 \times 10^{-3} \pm 8.6 \times 10^{-4}$
A_{15}	$8.88 \times 10^{-4} \pm 3.7 \times 10^{-5}$
A_{30}	$6.54 \times 10^{-4} \pm 1.4 \times 10^{-5}$
C_3	$1.31 \times 10^{-3} \pm 1.2 \times 10^{-4}$
C_6	$1.21 \times 10^{-3} \pm 2.1 \times 10^{-4}$
C_{15}	$6.94 \times 10^{-4} \pm 2.6 \times 10^{-5}$
C_{30}	$3.34 \times 10^{-4} \pm 1.4 \times 10^{-5}$
G_{15}	$2.04 \times 10^{-3} \pm 2.7 \times 10^{-5}$
T_3	$2.23 \times 10^{-3} \pm 4.2 \times 10^{-4}$
T_6	$1.81 \times 10^{-3} \pm 5.3 \times 10^{-4}$
T_{15}	$7.37 \times 10^{-4} \pm 4.2 \times 10^{-5}$
T_{30}	$3.81 \times 10^{-4} \pm 3.0 \times 10^{-5}$
A_3T_3	$1.84 \times 10^{-3} \pm 1.9 \times 10^{-4}$
C_3A_3	$1.83 \times 10^{-3} \pm 2.0 \times 10^{-4}$
C_3T_3	$1.38 \times 10^{-3} \pm 1.1 \times 10^{-4}$
G_3T_3	$3.44 \times 10^{-3} \pm 2.1 \times 10^{-4}$

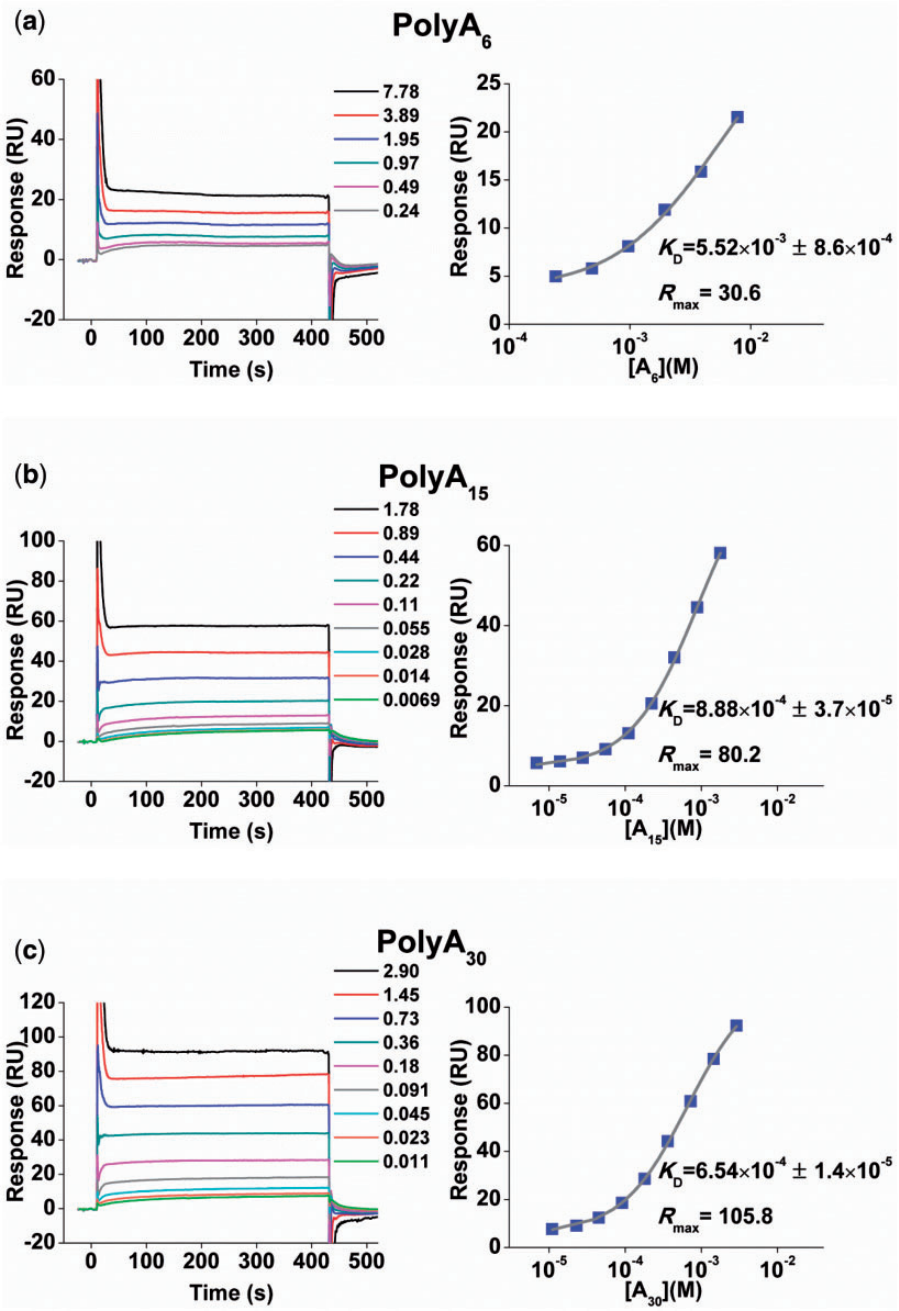

Fig. 2 Sensorgrams and binding analysis of immobilized L-methionine to oligonucleotides at 25°C. (**A**) polyA$_6$; (**B**) polyA$_{15}$; (**C**) polyA$_{30}$; (**D**) polyC$_3$; (**E**) polyC$_6$; (**F**) polyC$_{15}$; (**G**) polyC$_{30}$; (**H**) polyG$_{15}$; (**I**) polyT$_3$; (**J**) polyT$_6$; (**K**) polyT$_{15}$; (**L**) polyT$_{30}$; (**M**) polyA$_3$T$_3$; (**N**) polyC$_3$A$_3$; (**O**) polyC$_3$T$_3$; (**P**) polyG$_3$T$_3$. Concentrations in each sensorgram are given in mM.

oligonucleotides tested showed K_D values ranging from 0.3 to 5.5 mM (see Table II), which indicate low binding affinity. On the other hand, the L-histidine agarose support, which successfully purified sc pDNA (*18*), has lower K_D values (*27*) (ranged from 0.384 μM to 0.02 mM) compared to the results obtained in this study. However, in chromatography, the interaction occurs because conditions of high salt concentration are used, mainly to promote hydrophobic interactions, which prevail in both cases (*30*, *31*).

The sensorgrams and equilibrium binding analysis, at 25°C, fitted to a steady-state model for polyA6, polyA15, polyA30, polyC3, polyC6, polyC15, polyC30, polyG15, polyT3, polyT6, polyT15, polyT30 and CCCTTT, CCCAAA, GGGTTT, AAA TTT are presented in Fig. 2.

The highest binding affinity was found for polyC$_{30}$ ($3.34 \times 10^{-4} \pm 1.4 \times 10^{-5}$ M), followed by polyT$_{30}$ ($3.81 \times 10^{-4} \pm 3.0 \times 10^{-5}$ M) and polyA$_{30}$ ($6.54 \times 10^{-4} \pm 1.4 \times 10^{-5}$ M), while polyA$_6$ ($5.52 \times 10^{-3} \pm 8.6 \times 10^{-4}$ M) showed the lowest affinity to the L-methionine surface, followed by polyT$_3$ ($2.23 \times 10^{-3} \pm 4.2 \times 10^{-4}$ M) and polyG$_{15}$ ($2.04 \times 10^{-3} \pm 2.7 \times 10^{-5}$ M). The maximum RU signal was higher for

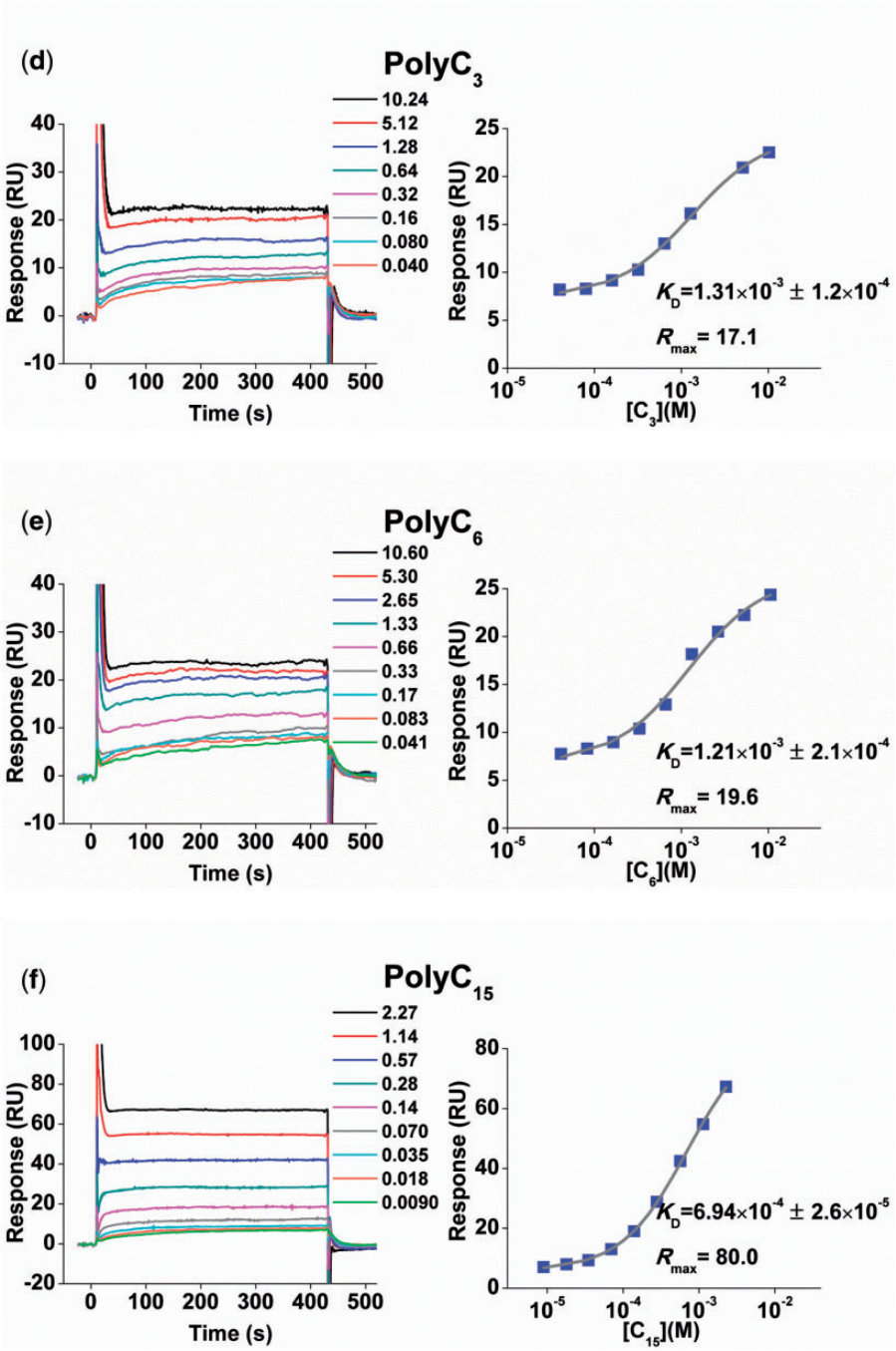

Fig. 2 Continued.

oligonucleotides with 30 bases and backbone (Fig. 2), suggesting that an increase in the number of bases and backbone leads to a higher binding affinity to the L-methionine surface. For 5′-mononucleotides experiments, no binding response was detected.

For poly15, the order of K_D values was $polyG_{15}$ ($2.04 \times 10^{-3} \pm 2.7 \times 10^{-5}$ M) > $polyA_{15}$ ($8.88 \times 10^{-4} \pm 3.7 \times 10^{-5}$ M) > $polyT_{15}$ ($7.37 \times 10^{-4} \pm 4.2 \times 10^{-5}$ M) ≈ $polyC_{15}$ ($6.94 \times 10^{-4} \pm 2.6 \times 10^{-5}$ M), with $polyC_{15}$ and $polyT_{15}$ showing the highest affinity (Table II). For poly30 and poly6, the order of K_D values was also the same (polyA > polyT ≈ polyC). For poly3, polyC showed higher affinity than polyT. Generally, there were slight differences in K_D values of polyC and polyT on L-methionine surface. The strongest interaction obtained with larger nucleotides could be attributed to their higher hydrophobic degree that allows more interactions per surface area, inducing cooperative effects and increasing the stability of the interaction. These results are in stark agreement with previous affinity data reported using L-arginine, L-lysine and L-histidine immobilized on the surface (*26*, *27*), that have similar binding affinities (10^{-4} to 10^{-3} M range) (*26*), except for L-histidine, whose K_D values ranged from 10^{-7} to 10^{-5} (*27*). However, the $polyT_3$ showed higher affinity for the L-methionine surface

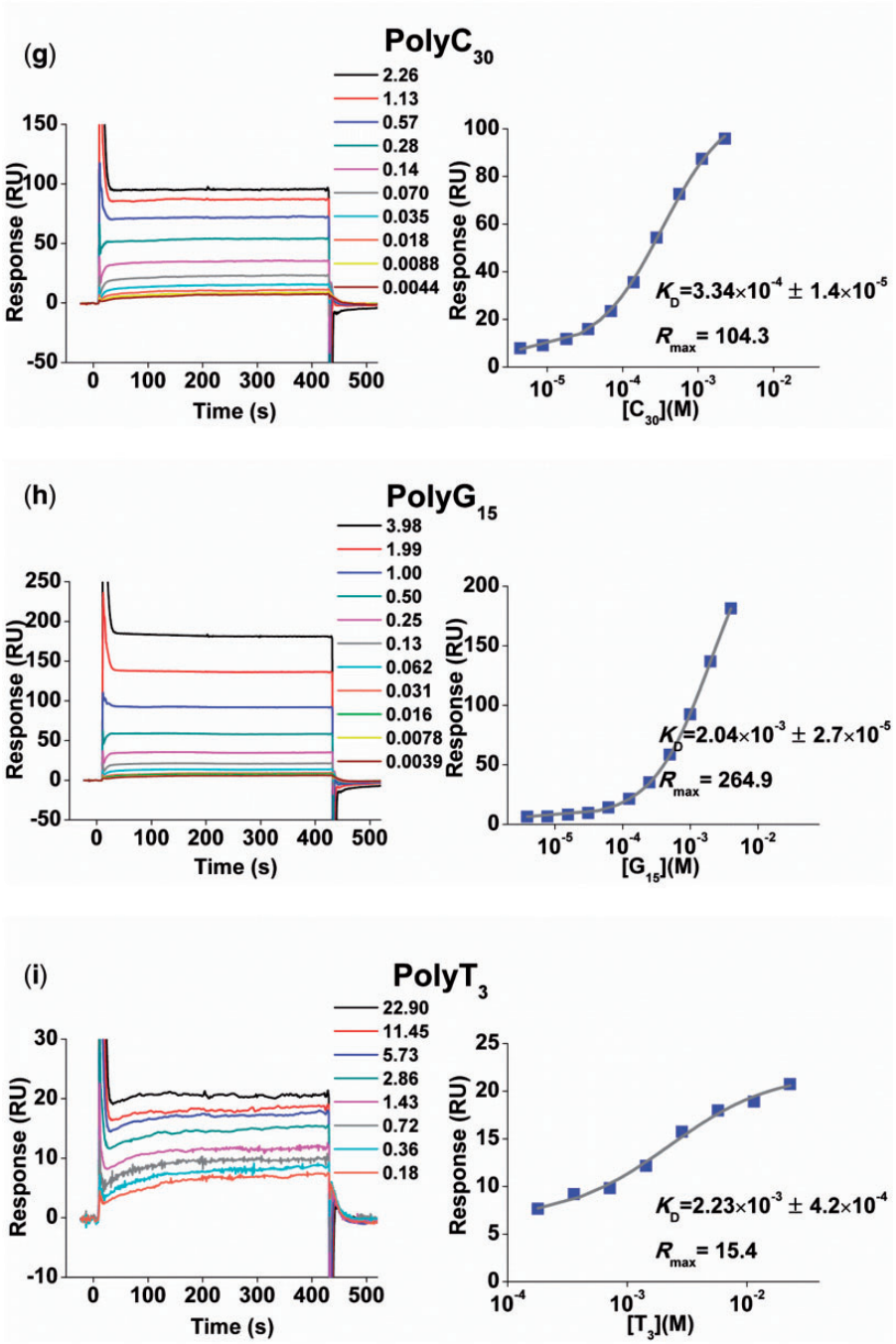

Fig. 2 Continued.

than $polyA_6$. This can be explained by the fact that thymine have a higher binding preference to L-methionine than adenine. This can be attested by NMR studies that recognized L-methionine to interact preferentially with thymine (*30*). Although the chromatographic conditions used to purify nucleic acids in L-methionine and L-histidine supports are the same (high salt concentration to promote nucleic acids retention), L-methionine has preference for pyrimidines (T and C), whereas L-histidine has preference for purines (A and G) (*31*).

The $polyA_6$–$polyA_{30}$ series showed a binding increase of 8.4-fold on the L-methionine surface. On the contrary, a previous work describes lower binding increase with L-arginine and L-lysine surfaces (3.7-fold and 1.7-fold, respectively). For $polyT_3$–$polyT_{15}$ series, higher binding increase was found for L-arginine surface (15-fold) using the same conditions (*26*). Thus, when the length of oligonucleotides increases, the binding affinity also increases and is more pronounced for polyA and polyT to L-methionine derivative and L-arginine, respectively. For $polyC_3$ and $polyC_{15}$, the binding increase on the L-methionine surface was negligible (1.8-fold). For the $polyT_3$–$polyT_{30}$ series, binding increased 5.9-fold for L-methionine surface, representing a twice increase in affinity when the number of nucleotides also

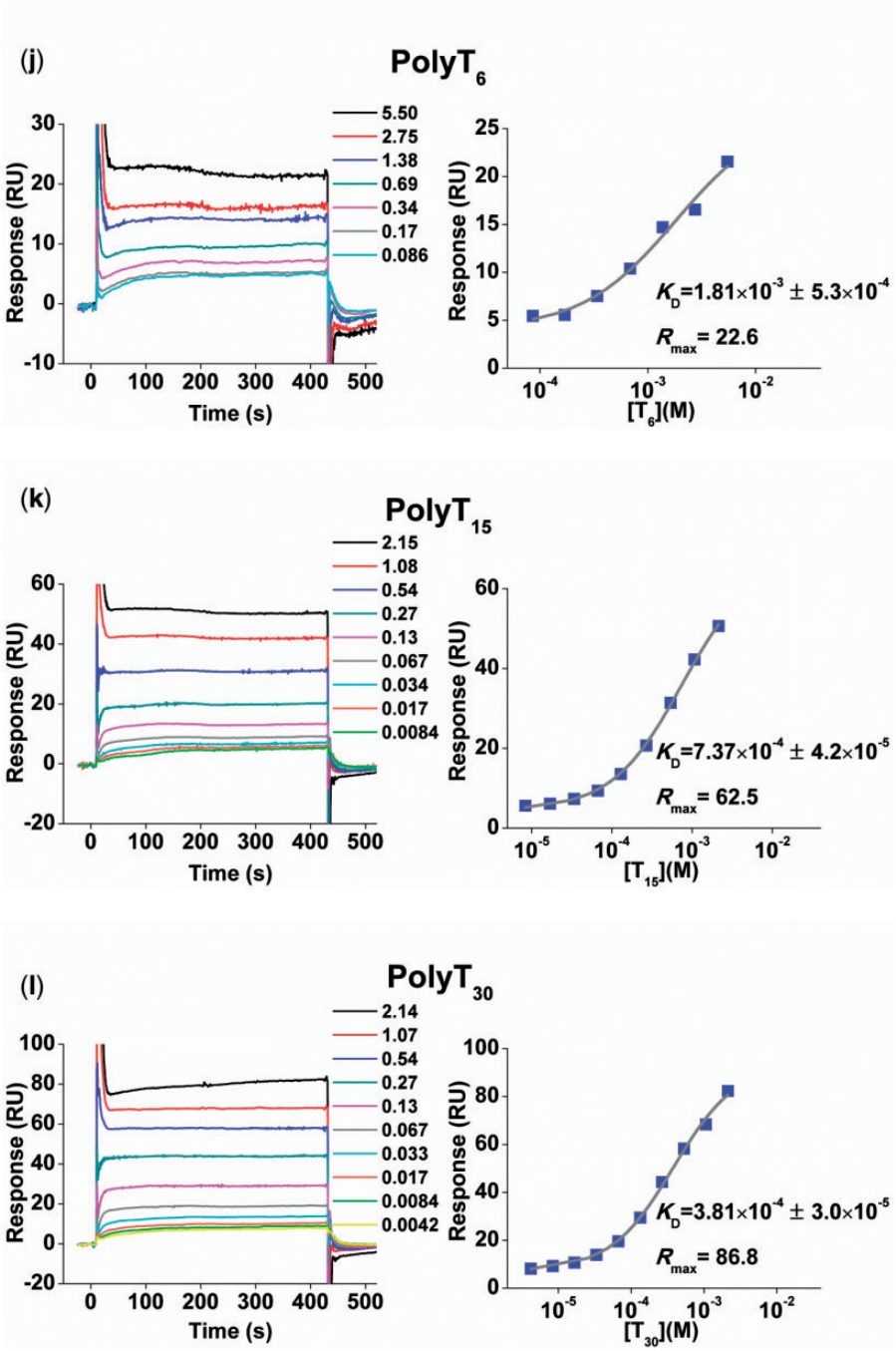

Fig. 2 Continued.

increases to double (3.0-fold for polyT$_3$–polyT$_{15}$ series). For polyC$_3$–polyC$_{30}$ series, binding affinity to L-methionine increased 3.9-fold, whereas for polyC$_3$–polyC$_{15}$ series, binding increased 1.8-fold.

K_D value of polyC$_6$ for L-methionine ($1.21 \times 10^{-3} \pm 2.1 \times 10^{-4}$ M) was nearly the same for L-arginine ($1.33 \times 10^{-3} \pm 0.05$ M) and for L-lysine surfaces ($1.76 \times 10^{-3} \pm 0.04$ M) (*26*).

In general, the L-methionine support showed to be ideal to interact with the hydrophobic bases, which is in accordance with previously reported studies done by STD-NMR and chromatographic experiments (*26*). Our group also suggested, by chromatographic experiments, that base composition could also be responsible for specific interactions of L-methionine support with thymine (*30*).

The maximum binding affinity between oligonucleotides and immobilized L-methionine was found for cytosine and thymine followed by adenine, whereas the lowest binding was observed for guanine. In this study it was not possible to mimic completely the L-methionine agarose support, as L-methionine ligand was immobilized through their reactive ester on the surface leaving the amino group free to interact with

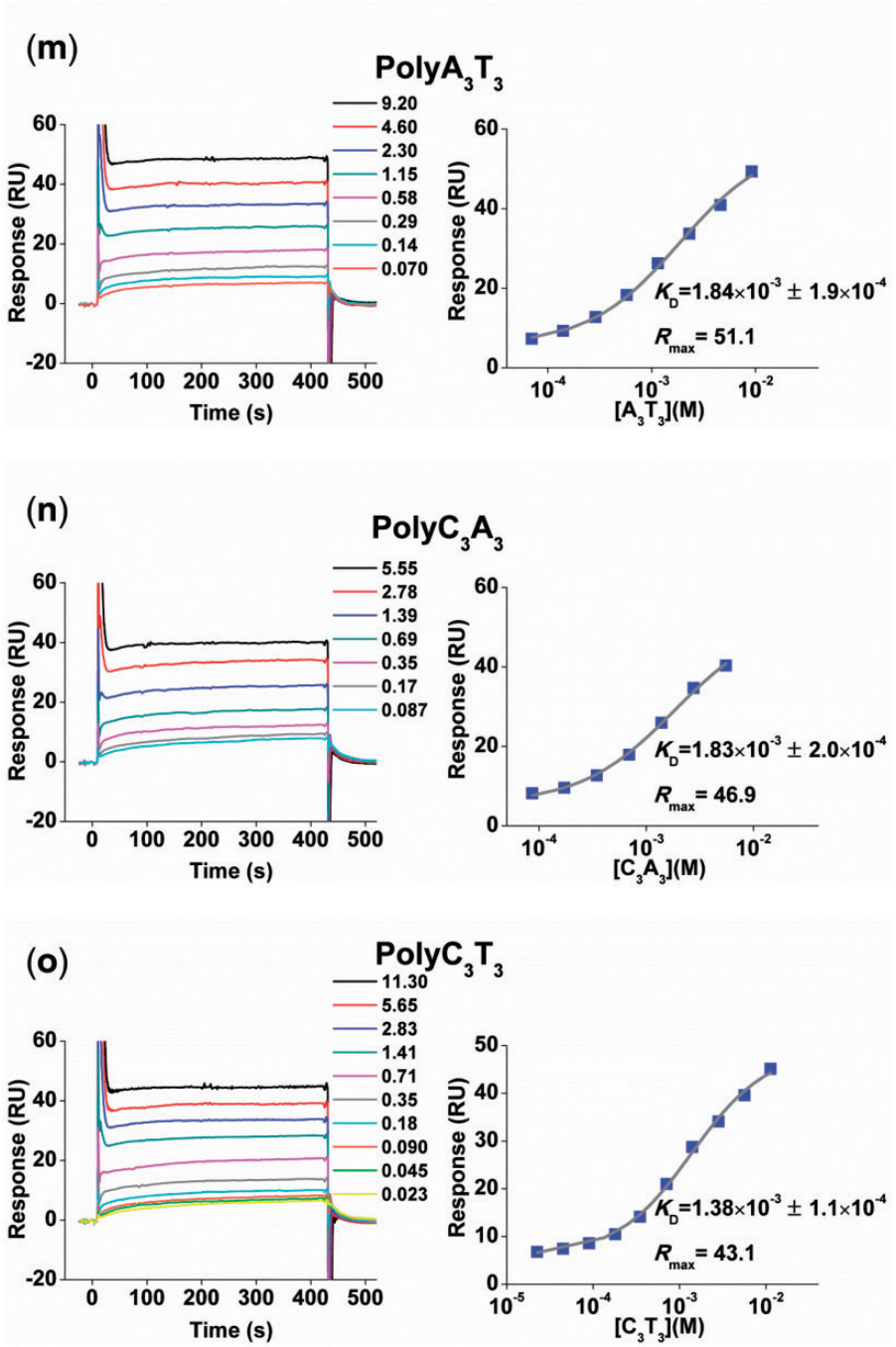

Fig. 2 Continued.

oligonucleotide. Nevertheless, these findings are consistent with a previous affinity chromatographic study using the L-methionine-agarose (*30*), in which thymine base presented a stronger retention in the support. Thus, it is possible to verify that this reverse approach (amine group free to interact with different oligonucleotides) did not change the affinity of L-methionine to the oligonucleotides.

An analysis of the contacts observed in amino acid residues and DNA complexes from crystal structures shows that L-methionine has preferential contacts with thymine/cytosine ≥ adenine (*6*). The single methyl group of the thymine base is the main target for hydrophobic interaction (*14*). The two CH groups of the cytosine base are also possible targets for recognition by hydrophobic residues. However, interaction with the hydrogen atoms of cytosine will not be as strong as with the methyl group of thymine (*6*). Furthermore, L-methionine has H-bond acceptor, forming H-bonds with the adenine or cytosine bases (*6*, *20*).

The effect of nucleotide composition on the binding of hetero-oligonucleotides (CCCTTT, CCCAAA, GG

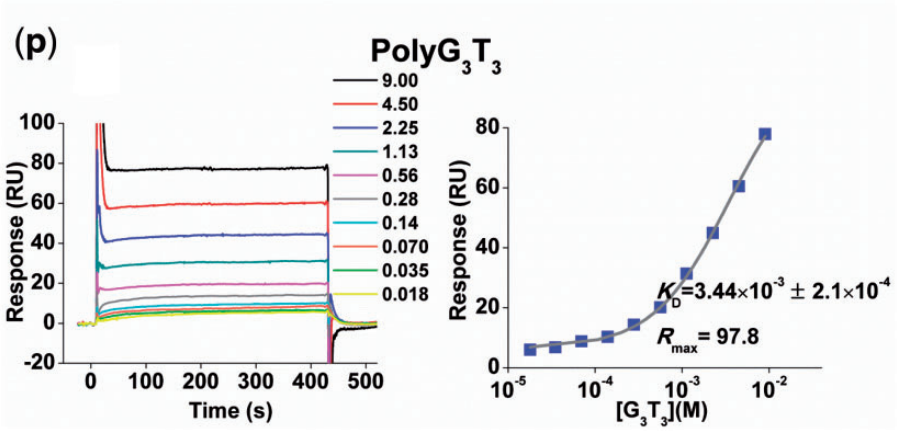

Fig. 2 Continued.

GTTT and AAATTT) to L-methionine surface was also evaluated. The K_D order was GGGTTT > AAA TTT ≈ CCCAAA ≈ CCCTTT (Table II). There were negligible differences between equilibrium K_D values determined for AAATTT, CCCAAA and CCCTTT.

The affinity decreased 2-fold when the hetero-oligonucleotide has three guanines. On the other hand, the affinity increased slightly (1.3-fold) when three nucleotides of polyT$_6$ were changed by three cytosines ($K_D = 1.38 \times 10^{-3} \pm 1.1 \times 10^{-4}$). When three nucleotides of polyT$_6$ were changed by three adenines the affinity was nearly the same (K_D of $1.84 \times 10^{-3} \pm 1.9 \times 10^{-4}$ M). Regarding to polyC$_6$, the affinity decreased slightly when three nucleotides were changed by three thymines (K_D values from $1.21 \times 10^{-3} \pm 2.1 \times 10^{-4}$ to $1.38 \times 10^{-3} \pm 1.1 \times 10^{-4}$ M) or by three adenines (K_D of $1.83 \times 10^{-3} \pm$;2.0×10^{-4} M). Still, the affinity increased 3-fold when three nucleotides of polyA$_6$ were changed by three cytosines (K_D values from $5.52 \times$;$10^{-3} \pm 8.6 \times 10^{-4}$ to $1.83 \times 10^{-3} \pm 2.0 \times 10^{-4}$) or by three thymines ($K_D$ $1.84 \times 10^{-3} \pm 1.9 \times 10^{-4}$ M). Thus, the cytosine and thymine bases in the oligonucleotide sequences increase the affinity with the L-methionine derivative. Furthermore, it can be seen that a combination of cytosine and thymine bases exhibit the highest affinity. On the other hand, the GGGTTT was the hetero-oligonucleotide that displayed the lowest affinity, showing that the presence of guanine reduces the affinity with the L-methionine immobilized.

SPR measurements were successfully used to screen affinity data between L-methionine derivative and oligonucleotides emphasizing that this ligand established preferential interactions with cytosine and thymine.

Conclusion

The development of safer, more effective and economic therapeutic approaches needs the development of robust, efficient and potential chromatographic supports. Therefore, it is necessary to find new specific ligands for the industrial purification of DNA biopharmaceuticals.

In light of these considerations, L-methionine derivative was synthesized and a strategy to immobilize it was presented. This ligand had the amino group free to interact with the oligonucleotides. Their binding affinity was evaluated to synthetic homo-oligonucleotides (with sizes up to 30 bases) and hetero-oligonucleotides by SPR biosensor. The highest binding affinity was found for cytosine and thymine bases, followed by adenine, while the lowest affinity was found for the guanine base. Moreover, the additional analysis with hetero-oligonucleotide also showed that the composition affected the interaction strength with an increase in response for oligonucleotides containing cytosine and thymine and a marked decrease for oligonucleotides containing guanine. From this study we conclude that this ligand interact preferential with hydrophobic bases.

Conflict of Interest

None declared.

Acknowledgements

This work was supported by FCT, the Portuguese Foundation for Science and Technology (PTDC/EBB-BIO/114320/2009), PEst-C/SAU/UI0709/2011 COMPETE and FCOMP-01-0124-FEDER-041068—Ref[a]. EXPL/QEQ-MED/1068/2013. E. Mota acknowledges a fellowship (CENTRO-07-ST24-FEDER-002014) from 'Programa Operacional Regional do Centro 2007-2013 QREN' ('Mais Centro' program). C. Cruz also acknowledges a post-doctoral grant from FCT (SFRH/BPD/46934/2008).

References

1. Babu, M.M., Luscombe, N.M., Aravind, L., Gerstein, M., and Teichmann, S.A. (2004) Structure and evolution of transcriptional regulatory networks. *Curr. Opin. Struct. Biol.* **14**, 283–291
2. Lejeune, D., Delsaux, N., Charloteaux, B., Thomas, A., and Brasseur, R. (2005) Protein-nucleic acid recognition: statistical analysis of atomic interactions and influence of DNA structure. *Proteins* **61**, 258–271
3. Siggers, T.W., Silvok, A., and Honig, B. (2005) Structural alignment of protein-DNA interfaces: insights

into the determinants of binding specificity. *J. Mol. Biol.* **345**, 1027–1045
4. Hégarat, N., François, J.C., and Praseuth, D. (2008) Modern tools for identification of nucleic acid-binding proteins. *Biochimie* **90**, 1265–1272
5. Ashworth, J. and Baker, D. (2009) Assessment of the optimization of affinity and specificity at protein-DNA interfaces. *Nucleic Acids Res.* **37**, e73
6. Suzuki, M. (1994) A framework for the DNA-protein recognition code of the probe helix in transcription factors: the chemical and stereochemical rules. *Structure* **2**, 317–326
7. Marabotti, A., Spyrakis, F., Facchiano, A., Cozzini, P., Alberti, S., Kellogg, G.E., and Mozzarelli, A. (2008) Energy-based prediction of amino acid-nucleotide base recognition. *J. Comput. Chem.* **29**, 1955–1969
8. Luscombe, N.M., Laskowski, R.A., and Thornton, J.M. (2001) Amino acid-base interactions: a three-dimensional analysis of protein-DNA interactions at an atomic level. *Nucleic Acids Res.* **29**, 2860–2874
9. Hoffman, M.M., Khrapov, M.A., Cox, J.C., Yao, J., Tong, L., and Ellington, A.D. (2004) AANT: the Amino Acid-Nucleotide Interaction Database. *Nucleic Acids Res.* **32**, D174–D181
10. Bahadur, R.P., Zacharias, M., and Janin, J. (2008) Dissecting protein-RNA recognition sites. *Nucleic Acids Res.* **36**, 2705–2716
11. Segal, E. and Widom, J. (2009) From DNA sequence to transcriptional behavior: a quantitative approach. *Nat. Rev. Genet.* **10**, 443–456
12. Pabo, C.O. and Sauer, R.T. (1984) Protein DNA recognition. *Annu. Rev. Biochem.* **53**, 293–321
13. Sousa, F., Prazeres, D.M., and Queiroz, J.A. (2008) Affinity chromatography approaches to overcome the challenges of purifying plasmid DNA. *Trends Biotechnol.* **26**, 518–525
14. Sousa, F., Cruz, C., and Queiroz, J.A. (2010) Amino acids-nucleotides biomolecular recognition: from biological occurrence to affinity chromatography. *J. Mol. Recognit.* **23**, 505–518
15. Lowe, C.R., Lowe, A.R., and Gupta, G. (2001) New developments in affinity chromatography with potential application in the production of biopharmaceuticals. *J. Biochem. Biophys. Methods* **49**, 561–574
16. Diogo, M.M., Queiroz, J.A., and Prazeres, D.M. (2005) Chromatography of plasmid DNA. *J. Chromatogr. A* **1069**, 3–22
17. Platonova, G.A. and Tennikova, T.B. (2005) Chromatographic investigation of macromolecular affinity interactions. *J. Chromatogr. A* **1065**, 75–81
18. Sousa, F., Freitas, S., Azzoni, A.R., Prazeres, D.M., and Queiroz, J.A. (2006) Selective purification of supercoiled plasmid DNA from clarified cell lysates with a single histidine-agarose chromatography step. *Biotechnol. Appl. Biochem.* **45**, 131–140
19. Sousa, F., Prazeres, D.M., and Queiroz, J.A. (2007) Dynamic binding capacity of plasmid DNA in histidine-agarose chromatography. *Biomed. Chromatogr.* **21**, 993–998
20. Coulocheri, S.A., Pigis, D.G., Papavassiliou, K.A., and Papavassiliou, A.G. (2007) Hydrogen bonds in protein-DNA complexes: where geometry meets plasticity. *Biochimie* **89**, 1291–1303
21. Oda, M. and Nakamura, H. (2000) Thermodynamic and kinetic analyses for understanding sequence-specific DNA recognition. *Genes Cells* **5**, 319–326
22. Myszka, D.G., Jonsen, M.D., and Graves, B.J. (1998) Equilibrium analysis of high affinity interactions using BIACORE. *Anal. Biochem.* **265**, 326–330
23. Day, Y.S., Baird, C.L., Rich, R.L., and Myszka, D.G. (2002) Direct comparison of binding equilibrium, thermodynamic, and rate constants determined by surface- and solution-based biophysical methods. *Protein Sci.* **11**, 1017–1025
24. Chiorcea Paquim, A.M., Oretskaya, T.S., and Oliveira Brett, A.M. (2006) Adsorption of synthetic homo- and hetero-oligodeoxynucleotides onto highly oriented pyrolytic graphite: atomic force microscopy characterization. *Biophys. Chem.* **121**, 131–141
25. Lu, K., Li, R., and Ma, L. (2008) Investigation on interaction of L-methionine dipeptide with ct-DNA by ultraviolet spectroscopy. *Phosphorus Sulfur Silicon Relat. Elem.* **183**, 596–602
26. Cruz, C., Cabrita, E.J., and Queiroz, J.A. (2011) Screening nucleotide binding to amino acid-coated supports by surface plasmon resonance and nuclear magnetic resonance. *Anal. Bioanal. Chem.* **401**, 983–993
27. Cruz, C., Santos, S.D., Cabrita, E.J., and Queiroz, J.A. (2013) Binding analysis between L-histidine immobilized and oligonucleotides by SPR and NMR. *Int. J. Biol. Macromol.* **56**, 175–180
28. Cruz, C., Sousa, A., Sousa, F., and Queiroz, J.A. (2013) Affinity analysis between immobilized L-arginine and plasmid isoforms provided by surface plasmon resonance. *Anal. Methods* **5**, 1682–1686
29. Cruz, C., Sousa, A., Mota, E., Sousa, F., and Queiroz, J.A. (2014) Quantitative analysis of histamine- and agmatine-DNA interactions using surface plasmon resonance. *Int. J. Biol. Macromol.* **70**, 131–137
30. Cruz, C., Sousa, A., Sousa, F., and Queiroz, J.A. (2012) Study of the specific interaction between L-methionine chromatography support and nucleotides. *J. Chromatogr. B Analyt. Technol. Biomed. Life Sci.* **909**, 1–5
31. Sousa, A., Sousa, F., Prazeres, D.M.F., and Queiroz, J.A. (2009) Histidine affinity chromatography of homo-oligonucleotides. Role of multiple interactions on retention. *Biomed. Chromatogr.* **23**, 745–753